Phys. Status Solidi A **209**, No. 3, 439–442 (2012) / **DOI** 10.1002/pssa.201100376

physica status solidi a
www.pss-a.com
applications and materials science

Current–voltage characteristics of cubic Al(Ga)N/GaN double barrier structures on 3C–SiC

C. Mietze[*], K. Lischka, and D. J. As

Department of Physics, University of Paderborn, Warburger Str. 100, 33098 Paderborn, Germany

Received 8 July 2011, revised 4 November 2011, accepted 4 November 2011
Published online 27 December 2011

Keywords cubic nitrides, molecular beam epitaxy, negative differential resistance, resonant tunnelling diodes

[*] Corresponding author: e-mail cmietze@mail.upb.de, Phone: +49 5251 60 5828, Fax: +49 5251 60 5843

Resonant tunnelling diodes of cubic Al(Ga)N/GaN were grown by plasma assisted molecular beam epitaxy on 3C-SiC (001). We observe a pronounced negative differential resistance at about 1.2 V with a peak-to-valley ratio (PVR) of 1.3 to 2.7 at room temperature. Experimental data is in good agreement with calculated *I–V* curves showing only a small deviation of 0.3 V of the resonance peak voltage. We find a decrease of the PVR when the *I–V* characteristic is measured repeatedly with short time intervals between the voltage-cycles. However, the *I–V* characteristics can be recovered fully when the diodes are illuminated by UV-light indicating charge trapping in our devices. Mesa structures are prepared by reactive ion etching. The size of the top ohmic contacts is $(25 \times 11)\,\mu m^2$. The Al content of the barrier material is varied between 30% and 100%.

1 Introduction Resonant tunnelling through double barrier structures is not only representing one of the most interesting phenomena in quantum mechanics but also very important for the understanding of current transport through heterostructures or superlattices. A general understanding of tunnelling through double barrier structures or superlattices is of crucial importance for the design and development of optoelectronic intersubband devices like quantum well infrared photodetectors (QWIP) or quantum cascade lasers (QCL). Group III-nitrides like GaN, AlN and their alloys are materials of high interest for optoelectronic devices or high power devices operating at high temperatures. In hexagonal GaN and AlN strong intrinsic piezoelectric and pyroelectric fields are present at the heterointerfaces. These built-in fields are undesirable for optical devices like QWIP or QCL [1]. Growth of the meta-stable cubic phase of GaN (c-GaN) and AlN (c-AlN) is a possibility to avoid these built-in fields, because of the cubic crystal symmetry [2]. Cubic group III-nitrides offer large potential for intersubband devices due to their large band offset [3] and non-polarity. During the last years a lot of progress in the fabrication of cubic III-nitride intersubband devices was made. In 2011 Machhadani et al. [4] showed intersubband absorption in the near infrared and terahertz spectral range. After resonant tunnelling has been successfully shown in the hexagonal group III-nitrides like in Ref. [5, 6], recently resonant tunnelling through cubic GaN/AlGaN double barriers on GaAs has been demonstrated [7], offering plenty of phenomena, which can be studied in cubic nitrides in the future.

2 Experimental Our samples were grown by plasma assisted molecular beam epitaxy (PA-MBE) on freestanding n-type cubic silicon carbide (3C-SiC). All resonant tunnelling diodes (RTD) consist of a highly doped 50 nm thick c-GaN buffer layer doped with silicon (Si). Doping concentration was $5 \times 10^{19}\,cm^{-3}$ for all samples, respectively. The buffer layer is followed by the resonant tunnelling structure. The tunnelling structure consists of a 1 nm thick unintentionally doped (uid) c-GaN quantum well (QW) embedded in two Al(Ga)N barriers which are unintentionally doped as well. The barrier thickness was varied between 1 and 3 nm while the Al-content in the barrier was 100% for sample A and 30% for samples B and C. The structural properties of the tunnelling structures are given in Table 1. Layer thicknesses were measured *in-situ* by reflection high-energy electron diffraction (RHEED) and growth rate calculations with accuracy of one monolayer. The double barrier structure was then capped by another highly doped 30 nm thick c-GaN cap layer. Furthermore, the double barrier structure was separated from the highly doped regions by 2 nm unintentionally doped c-GaN spacer layers to avoid interdiffusion of Si doping. After growth a mesa

Table 1 List of samples.

sample	barrier material	barrier thickness	PVR
A	AlN	3 nm	2.1
B	$Al_{0.3}Ga_{0.7}N$	1 nm	1.3
C	$Al_{0.3}Ga_{0.7}N$	2 nm	2.7

structure was fabricated using UV-photolithography and reactive ion etching (RIE). On top of the mesa structure the ohmic top contact was deposited by thermal evaporation of 15 nm Ti, 50 nm Al, 15 nm Ti and 50 nm Au. The size of the top contact is $(11 \times 25)\ \mu m^2$. The back contact is formed by indium on a copper plate. A schematic drawing of the RTD is shown in Fig. 1. No further thermal annealing of the contacts was performed to avoid interdiffusion of the Si-doping into the tunnelling structure. The fabricated devices were then characterized by dc current–voltage (*I*–*V*) measurements using an Agilent 4156C parameter analyser. The voltage was applied to the top contact while the current through the whole structure was measured. All measurements were performed in dc-mode with an integration time of 0.64 ms and a step size of 0.01 V at room temperature.

3 Results and discussion The *I*–*V* characteristics of three different devices revealed a clear NDR in forward bias direction. However, the resonance peak is only observed sweeping from zero bias to higher voltages and does not occur in the opposite direction. Furthermore, the *I*–*V* curve was asymmetrical as an effect of the hetero-junction between 3C-SiC and c-GaN. No NDR could be observed in negative bias direction. Hence, we will discuss only the forward bias direction in the following. In Fig. 2 the *I*–*V* characteristics of samples A, B and C are plotted for the first *I*–*V* measurement. The current was normalized for better comparability. Overall peak-to-valley ratios from 2.7 to 1.3 are observed. For

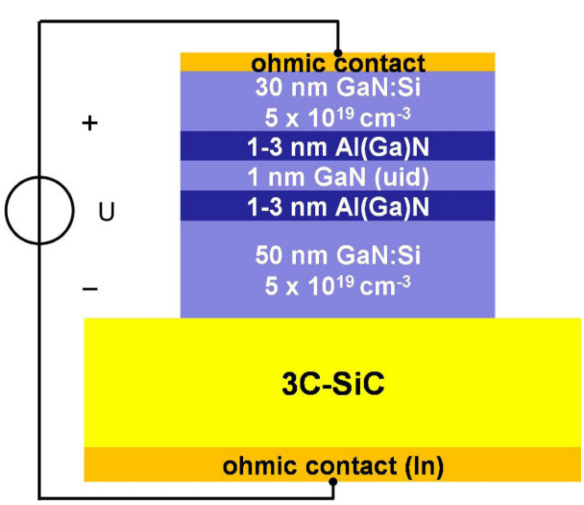

Figure 1 (online colour at: www.pss-a.com) Schematic drawing of the cubic Al(Ga)N/GaN resonant tunnelling diode structure.

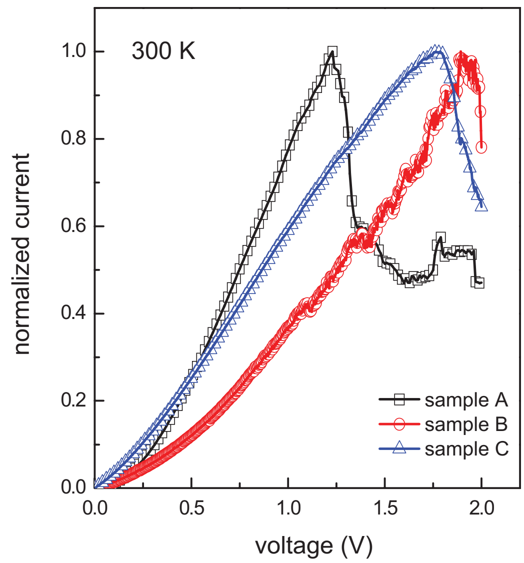

Figure 2 (online colour at: www.pss-a.com) Typical *I*–*V* characteristics of samples A, B and C for the first measurement.

samples with AlGaN barriers the resonance peak occurs at higher bias voltage than for sample A, although for sample A the confinement energy is larger due to larger band offset between barriers and QW. This is an effect of higher contact resistances of the different samples since the contacts were not thermal annealed in order to avoid interdiffusion in the tunnelling structure. Furthermore, the *I*–*V* curves of samples B and C do not reach the current valley because no bias voltages larger than 2 V were applied in the first measurement in order to protect the sample from being damaged by too high current densities. Furthermore, the tunnelling characteristics have been modelled using nextnano [3]. The *I*–*V* characteristics as well as electron densities were calculated using the contact block reduction method (CBR). More information about the theoretical model can be found in Ref. [8]. In Fig. 3, the calculated *I*–*V* characteristic of sample A is plotted together with the measured values. The current densities have been normalized on the resonance peak value. Only a small deviation of the peak voltage between calculation and experimental data is observed. However, the deviation in the region below the resonance may be due to leakage current through conducting channels or non-resonant tunnelling which is not included in the calculation. Interface roughness and layer thickness fluctuations also influence the experimental results and lead to a broadening of the resonance peak. The calculated electron densities for three different bias voltages, below resonance, resonant tunnelling and off resonance are plotted in Fig. 4 together with the corresponding band structure. Only if the Fermi level is resonant with the localized state we find a remarkable density inside the quantum well. If bias voltage is further increased current transfer over the barrier structure occurs. When measuring the first *I*–*V* characteristics, we observed that the NDR vanishes after the first or second voltage sweep, which has been observed in the

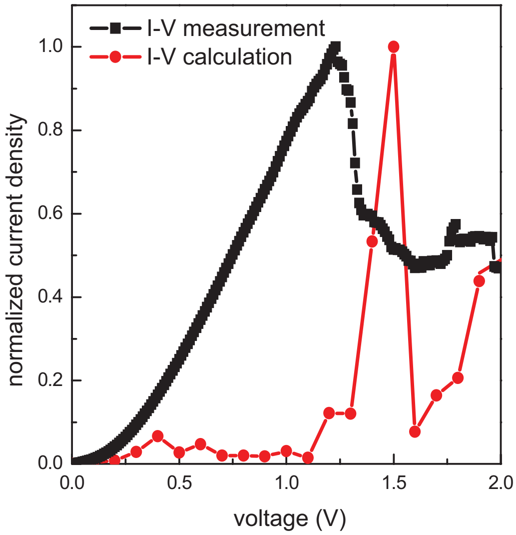

Figure 3 (online colour at: www.pss-a.com) Calculated *I–V* characteristic of sample A (red dots) in comparison to the measured *I–V* curve (black squares).

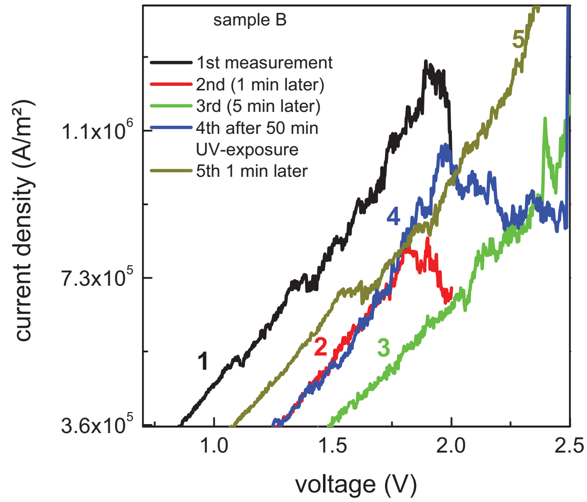

Figure 5 (online colour at: www.pss-a.com) Sequenced *I–V* characteristics of sample B with vanishing (green and dark yellow curve) and recovering (blue curve) negative differential resistance.

hexagonal system as well. In order to find the physical origin of this behaviour, we have illuminated the sample with UV-light. We used an UV-lamp, having its maximum intensity at a wavelength of 370 nm. After 1 h of UV-exposure the NDR could be recovered several times. In Fig. 5, *I–V* curves which have been measured before and after illumination are plotted. The first and second *I–V* curves show clear NDR which vanishes in the third sweep. After 1 h of UV-illumination the *I–V* characteristic is recovered and vanishes again in the fifth sweep, which is measured immediately after the fourth *I–V* curve. The same behaviour is found for other samples as well and is an indication for charge trapping as it is mentioned in Ref. [6] as well. Calculations of band structure and *I–V* characteristics assuming fixed charges at the AlGaN/GaN interface showing no NDR support this assumption. Another effect can be observed in subsequent *I–V* measurements. With increasing number of sweeps the peak-to-valley ratio decreases. Furthermore, the resonance peak shifts slightly to higher voltages. This effect has also been observed in hexagonal AlGaN/GaN double barrier diodes [6]. In Fig. 6 further *I–V* traces for sample B are plotted. We clearly observe the recovery of the NDR again additional to the flattening and shifting of the resonance peak for *I–V* sweep numbers six and eight. The decrease of the

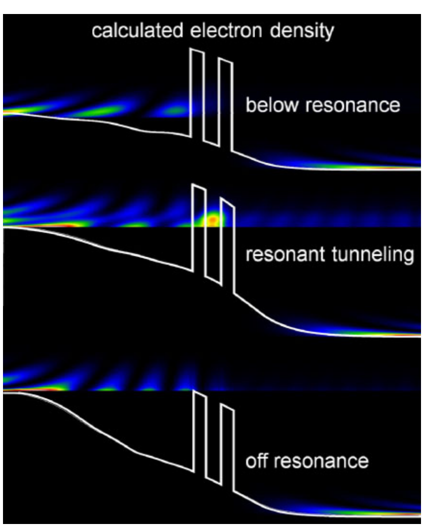

Figure 4 (online colour at: www.pss-a.com) Calculated electron density and corresponding band structure for three different bias voltages. Resonant tunnelling occurs for the case of high density inside the QW (middle).

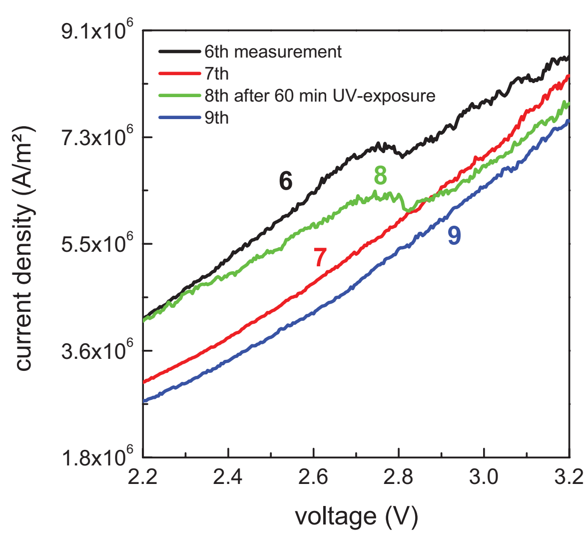

Figure 6 (online colour at: www.pss-a.com) Further *I–V* characteristics of sample B showing shifted NDR peak and decrease in peak-to-valley ratio.

PVR may be an indication for too low intensity of the UV-lamp. This effect has to be further investigated for spectral and intensity dependencies.

4 Conclusion RTDs with reproducible *I–V* characteristics and recoverable NDR based on Al(Ga)N/GaN double barrier structures were grown on free standing 3C-SiC (001) by PA-MBE. All devices show clear negative differential resistance with peak-to-valley ratios between 1.3 and 2.7. Furthermore, model calculations of the *I–V* characteristics and electron density were performed using nextnano [3] showing only a small deviation of the resonance peak voltage of 0.3 V. After the first *I–V* measurements the PVR decreases but can be fully recovered by illuminating the samples with UV-light. We suppose that this effect is due to charge trapping in our device. This is supported by calculations of the *I–V* characteristics assuming fixed charges at the AlGaN/GaN interface showing no negative differential resistance.

Acknowledgements The financial support by the German Science Foundation (DFG, project As (107/4-1)) is acknowledged. The authors also want to thank H. Nagasawa and M. Abe, HOYA Corporation, SiC Development Center, Japan, for the supply of the freestanding 3C-SiC (001) substrates.

References

[1] O. Ambacher, R. Dimitrov, M. Stutzmann, B. E. Foutz, M. J. Murphy, J. A. Smart, J. R. Shealy, N. G. Weimann, K. Chu, M. Chumbes, B. Green, A. J. Sierakowski, W. J. Schaff, and L. F. Eastman, Phys. Status Solidi A **216**, 381 (1999).
[2] D. J. As, Microelectron. J. **40**(2), 204 (2009).
[3] C. Mietze, M. Landmann, E. Rauls, H. Machhadani, S. Sakr, M. Tchernycheva, F. H. Julien, W. G. Schmidt, K. Lischka, and D. J. As, Phys. Rev. B **83**, 195301 (2011).
[4] H. Machhadani, M. Tchernycheva, L. Rigutti, S. Saki, R. Colombelli, C. Mietze, D. J. As, and F. H. Julien, Phys. Rev. B **83**, 075313 (2011).
[5] A. Kikuchi, R. Bannai, K. Kishino, C.-M. Lee, and J.-I. Chyi, Appl. Phys. Lett. **81**, 1729 (2002).
[6] S. Golka, C. Pflügl, W. Schrenk, C. Skierbiszewski, M. Siekacz, I. Grzegory, S. Porowski, and G. Strasser, Appl. Phys. Lett. **88**, 172106 (2006).
[7] N. Zainal, S. V. Novikov, C. J. Mellor, C. T. Foxon, and A. J. Kent, Appl. Phys. Lett. **97**, 112102 (2010).
[8] S. Birner, C. Schindler, P. Greck, M. Sabathil, and P. Vogl, J. Comput. Electron. **8**, 267 (2009).